

# Morphology and Mechanical Properties of Thermoplastic Elastomers from Nylon-Nitrile Rubber Blends

C. RADHESH KUMAR,<sup>1</sup> K. E. GEORGE,<sup>2</sup> and SABU THOMAS<sup>1,\*</sup>

<sup>1</sup>School of Chemical Sciences, Mahatma Gandhi University, Priyadarshini Hills, P.O., Kottayam-686 560, Kerala, India; and <sup>2</sup>Department of Polymer Science and Rubber Technology, Cochin University of Science and Technology, Cochin-22, Kerala, India

## SYNOPSIS

Nylon-nitrile rubber blends having different plastic-rubber component ratios (100/0, 80/20, 70/30, 60/40, 50/50, 40/60, 30/70, 20/80, and 0/100) were prepared by melt mixing technique in a Rheocord-90 at a temperature set at 180°C. The mixing characteristics of the blends have been analyzed from the rheographs. The morphology of the blend was studied using optical and electron microscopies, with special reference to the effect of blend ratio. The micrographs indicate a two-phase system where the component having lower proportions was found to disperse in the major continuous phase. A cocontinuous morphology was observed for 50/50 composition. Mechanical properties of the blends have been measured according to standard test methods. The effect of blend ratio on the mechanical properties like tensile strength, tear strength, elongation at break, stress-strain behavior, and hardness has been analyzed. The influence of the strain rate on the mechanical properties has also been analyzed. The mechanical properties were found to have a strong dependence on the amount of nylon in the blend. It is found that the blends with higher proportions of nylon have superior mechanical properties. The observed changes in mechanical properties are explained on the basis of the morphology of the blend. Various theoretical models such as Series, Parallel, Halpin-Tsai, and Coran's equations have been used to fit the experimental mechanical data. © 1996 John Wiley & Sons, Inc.

## INTRODUCTION

The blending of two or more polymers has gained considerable importance in recent years because the blends usually give rise to certain properties that cannot be attained from individual components. A good amount of research work has been carried out over the last several years with a view to obtain new polymeric materials with enhanced properties for specific application and for better combination of different properties. The thermoplastic elastomers from rubber-plastic blends are such materials that combine the excellent processing characteristics of the thermoplastic materials at high temperature and a wide range of physical properties of elastomers at

service temperature.<sup>1-5</sup> Thermoplastic elastomeric materials are reprocessible, and studies on this material are highly important due to their improved properties, easy processability, and economic advantages.

Nylon is a high modulus plastic having good mechanical strength, dimensional stability at elevated temperature, chemical resistance to many moderately polar and nonpolar organic species, and is a barrier to oxygen. However, it exhibits poor impact resistance especially at low temperature below  $T_g$  and in the dry state.<sup>6</sup> Nylons are used to blend with low modulus polymers such as rubbers<sup>7-10</sup> to improve impact properties. Nitrile rubber, on the other hand, is a special-purpose elastomer having good oil and abrasion resistance but poor ozone resistance. Blending of nylon with nitrile rubber produces a new class of material having excellent oil resistance, ozone resistance, good toughness, and mechanical

\* To whom correspondence should be addressed.

**Table I** Details of Materials Used

| Materials            | Characteristics  | Source                                      |
|----------------------|--|---|
| Nylon                | Appearance: clear uniform 2-mm chips<br>Density (g/cc): 1.11<br>Melting range (°C): 165–175<br>Water absorption (%) at 23°C: 10–12<br>Moisture regain (%): 2.5–3.5<br>Relative viscosity: 2.5–2.7      | SRF Ltd. (Madras, India)                    |
| Nitrile rubber (NBR) | Density (g/cc): 0.98<br>Volatile matter (%): 0.13<br>Antioxidant (%): 1.4<br>Organic acid (%): 0.25<br>Soap (%): 0.004<br>Bound acrylonitrile (%): 34<br>Mooney viscosity, ML <sub>1+4</sub> 100°C: 40 | Gujarat Apar Polymers Ltd., (Bombay, India) |

properties. It has been reported<sup>11–13</sup> by many authors that the properties of polymer blends depend on their morphology. Morphology of different polymer blends has been studied by various researchers.<sup>14–23</sup> A blend morphology wherein one component is dispersed within a continuum of the other has received great attention in literature. The strong influence of the morphology on the properties of the resulting polymer blends has been reported.<sup>24–26</sup> Cimmino and coworkers<sup>19</sup> have related the mechanical properties of binary polyamide 6/rubber blends with the blend morphology. Baer found mechanical and dynamic properties to be mainly dependent on the particle size.<sup>26</sup>

Two critical parameters for the toughening of polyamides are dispersed particle size and the interfacial adhesion. It has been shown that polyamide-rubber blends require a particle size less than 1  $\mu\text{m}$  to accomplish super toughness.<sup>7–10</sup> Borgreve and colleagues<sup>27–30</sup> reported that the impact behavior of the rubber-modified nylon depends on the type of modifier and their particle size. Coran and Patel<sup>31–35</sup> published a series of articles on rubber-thermoplastic blends correlating the physical properties of the blend with fundamental characteristics of the elastomer and thermoplastic components. Rheology, morphology, mechanical properties, and failure mode of various thermoplastic elastomer blends have been reported by De and coworkers.<sup>36–41</sup> Recently, Thomas and colleagues<sup>42–46</sup> have developed blends of ethylene vinyl acetate (EVA) with polypropylene and natural rubber. Miscibility, morphology, crystallization, mechanical properties, and aging behavior of these blends have been studied in detail.

In this paper, we report on the mechanical properties of nylon-nitrile rubber blends having various proportions of nylon and nitrile rubber prepared by melt blending technique. Attempts have been made to correlate the blend morphology with the observed mechanical properties. The influence of blend composition on morphology and mechanical properties have been analyzed. Finally, various theoretical models have been used to fit the experimental mechanical data.

## EXPERIMENTAL

### Materials

Nylon used in this work is a copolymer of nylon 6,6 and nylon 6, supplied by Sri Ram Fibres Ltd. (Madras, India). Nitrile rubber (Aparene N-553 NS) used in this work contains 34% bound acrylonitrile. The material was supplied by Gujarat Apar Ltd. (Bombay, India). The characteristics of the above materials are given in Table I.

### Preparation of the Blends and Test Samples

Blends of nylon and nitrile rubber (NBR) were prepared in a Rheocord-90 internal mixer with a rotor speed of 60 rpm; the total mixing time was fixed at 8 min. Nylon was melted first at a temperature of 180°C in the mixer and then NBR was added after 2 min. The blending was continued for 6 more min. The blend was taken out and compression molded at 180°C for 5 min into sheets 12 × 12 × 1.5 cm.

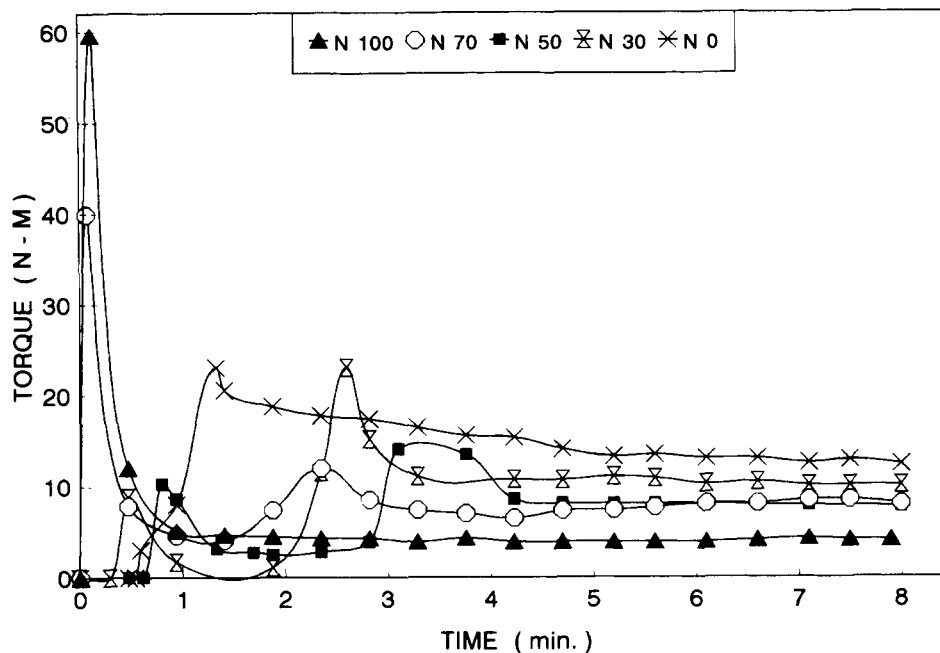


Figure 1 Rheographs showing time-torque relations.

Samples for tensile and tear tests are punched from the molded sheet. The blend ratios are denoted by  $N_{100}$ ,  $N_{80}$ ,  $N_{70}$ ,  $N_{50}$ ,  $N_{40}$ ,  $N_{30}$ ,  $N_{20}$ , and  $N_0$ . The subscripts denote the weight percentage of nylon in the blend.

#### Preparation of Samples for Morphology Studies

The molded samples of various blend ratios were broken after freezing them in liquid nitrogen. This has done to prevent the deformation of the phases during fracture. The NBR phase was preferentially extracted from the cryogenically fractured samples by keeping the broken edge in toluene for 2 weeks at room temperature. The NBR extracted samples were then dried in an air oven at  $40^{\circ}\text{C}$  for 24 h. The dried samples were then kept in a desiccator for the morphology studies. These samples were sputter coated with Au/Pd alloy, and scanning electron microscopy (SEM) studies were performed on a Philips-500 model scanning electron microscope. Optical microscopy was also used for morphology studies using (Leica Galen III) optical microscope.

#### Mechanical Properties

Before the mechanical testing, the test specimens were vacuum dried at  $70^{\circ}\text{C}$  for 3 h to remove the moisture. Tensile testing of the samples was performed at  $25 \pm 2^{\circ}\text{C}$  according to ASTM D412-80

test method using dumb-bell shaped test specimens at a crosshead speed of 500 mm/min using a Zwick Universal testing machine (model 1445). The tear strength was determined as per ASTM D624-81 using unnicked  $90^{\circ}$  angle test pieces. The experimental conditions of temperature and crosshead speed for the tear measurements are also the same as that of the tensile testing. The hardness of the samples was measured and expressed in shore D units. For hardness measurements, sheets having effective thickness 6 mm were used. The tensile set values after failure of the dumb-bell samples were determined according to ASTM D412-80. The influence of testing speed on the tensile and tear properties was also studied. The various crosshead speeds used were 5, 50, and 500 mm/min.

## RESULTS AND DISCUSSION

#### Processing Characteristics

The processing characteristics of the blend have been studied from the Rheocord-90 time-torque time-temperature curves, shown in Figures 1 and 2. These graphs are given to indicate the values of the torque and temperature under which the molten blends are mixed. Several authors have used the rheographs to analyze the processing characteristics of polymer blends.<sup>24,47,48</sup> The time-torque curves for

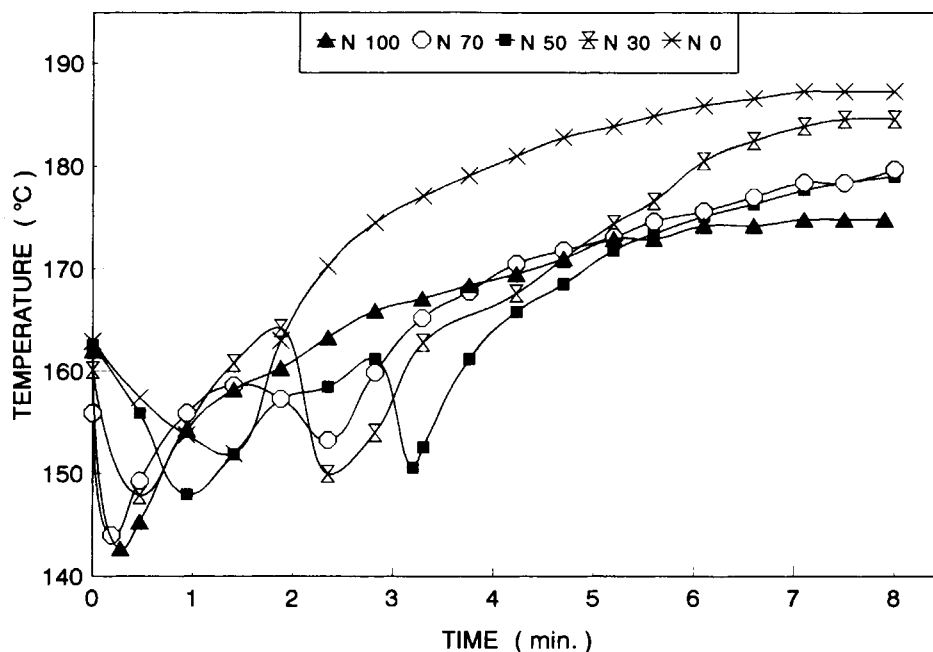


Figure 2 Rheographs showing time-temperature relations.

all blends have two peaks. The first peak is associated with increase in viscosity as a result of the introduction of unmolten nylon. The viscosity then decreases, showing the complete melting of nylon. Upon the addition of NBR into nylon, the viscosity again increases, which corresponds to the second peak. The curves thereafter come down, showing the complete melting of the second phase and finally curves level off to give uniform torque values at the end of the mixing cycle. The uniform torque value is an indication of good level of mixing of the two components. The extent of mixing is an important criteria for immiscible blends, because the final properties of the blend depend on the mixing time and extent of mixing. The torque values of the blend in general (after the addition of NBR) increases as the NBR content increases. The equilibrium mixing torque is maximum for NBR and is the lowest for nylon. The blends show intermediate behavior. This is attributed to the high melt viscosity of the NBR component compared with nylon. The large viscosity mismatch between NBR and nylon can lead to incompatibility and gross distribution of the minor phase in the major one. On the other hand, on polarity considerations, compatibility is favored due to the polar nature of NBR and nylon. However, the contribution of each factor toward compatibility/incompatibility could not be quantified.

Figure 2 shows the time-temperature mixing curves of the various nylon/NBR blends. The tem-

perature decreases first due to the introduction of plastic into the chamber and then increases showing the melting of the plastic. The second drop in temperature is due to the addition of NBR to the nylon melt. This drop is more pronounced for blends of high NBR content. The temperature again increases with time and levels off at the end of the mixing cycle. From the graph, it is clear that the mixing temperatures of the blends increase with increase in NBR content. This is due to the higher shear forces involved as NBR content increases, owing to its higher viscosity.

### Morphology of the Blends

Microscale morphology is a profound determinant of the properties of polymer blends. The prominent factors that decide the blend morphology are the blend ratio, the intrinsic melt viscosity of the components, shear rate during mixing, and the presence of additives such as fillers and plasticizers. It is reported that for the same processing conditions, the composition ratios and melt viscosity differences for the components determine the morphology.<sup>11</sup> If the viscosities of the components are matching, the dispersion of the minor phase is found to be uniform in the major phase. In cases of unmatching viscosities, the morphology depends on whether the minor component has a lower viscosity or higher viscosity than the major one. If the minor component has

lower viscosity, this component will be finely dispersed. In contrast, the minor component shows a coarse dispersion as spherical domains if its viscosity is higher than that of the major constituent.

The mode and state of dispersion of the domains are strongly dependent on the molecular structure and characteristics of the components, blend composition, blending procedure, and conditions of crystallization. The thermoplastic elastomers are phase-separated systems in which one phase is hard and solid, whereas the other phase is rubbery at room temperature. The hard phase acts as pseudo-cross-links. The strength in this system is provided by the hard phase, in the absence of which the elastomeric phase starts to flow under stress. The properties

usually depend on the amount of hard phase present. The elastomer phase controls the stability and stiffness of the resulting products. The maximized distribution of mixing stresses (due to viscosity matching) and generation of increased stresses (due to higher viscosities) would be expected to give more extensive break up of the dispersed phases. As can be seen later, in the present system of NBR dispersed blends, the large particle size is attributed to the difference between the surface energies of two phases. Several authors have attempted to correlate the morphology with the mechanical properties of the blends.<sup>11-13,36,41</sup> Avegeropoulos et al.<sup>49</sup> and Hamed<sup>50</sup> have studied the phase morphology developing during mixing. Initially, the dispersed phase

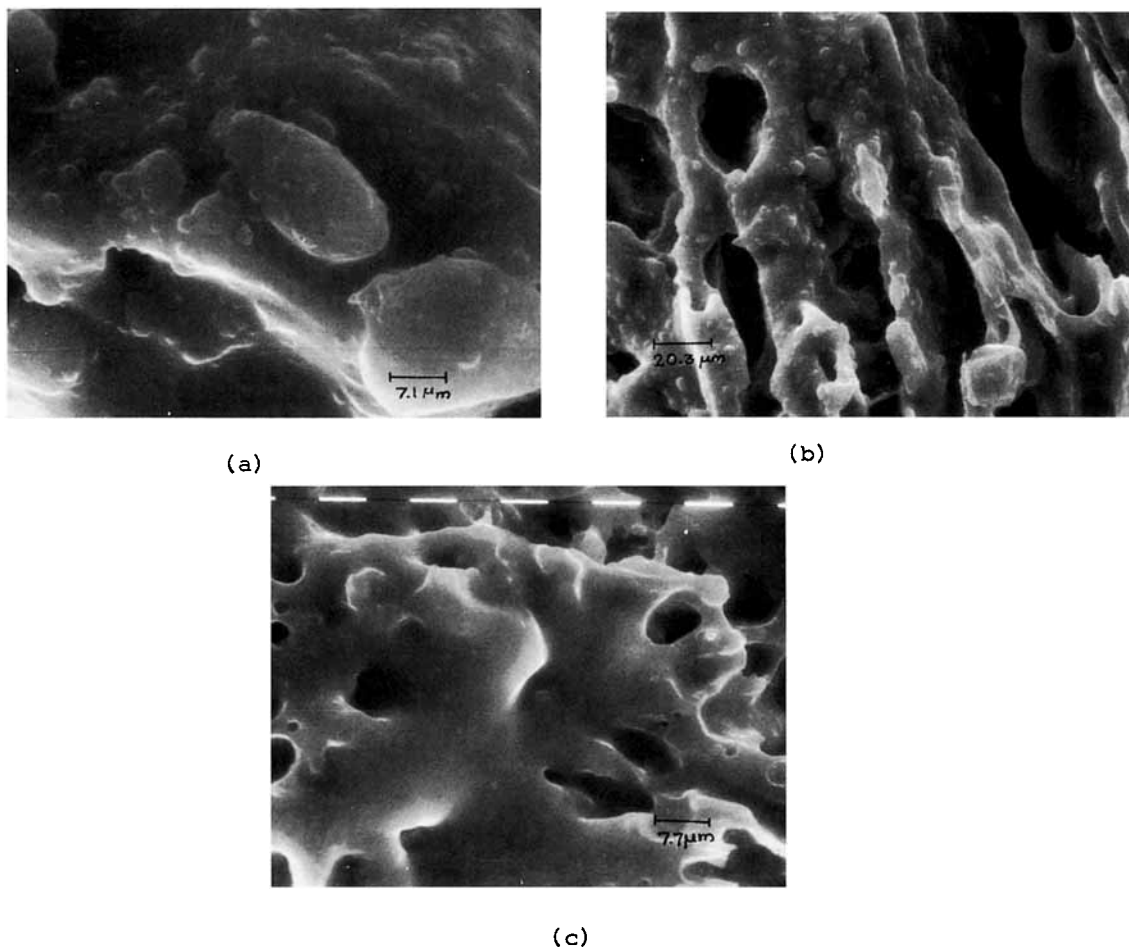
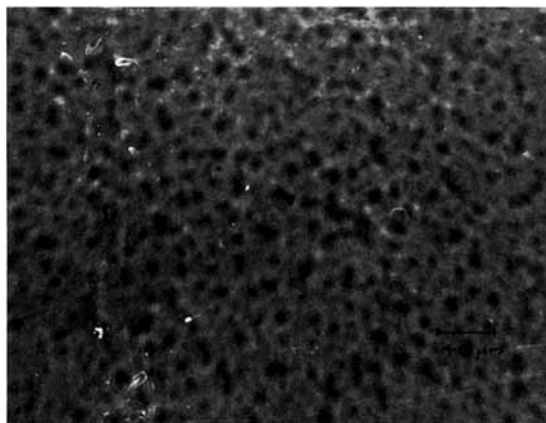
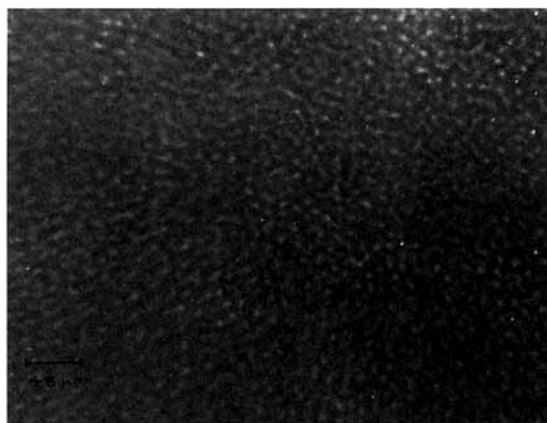


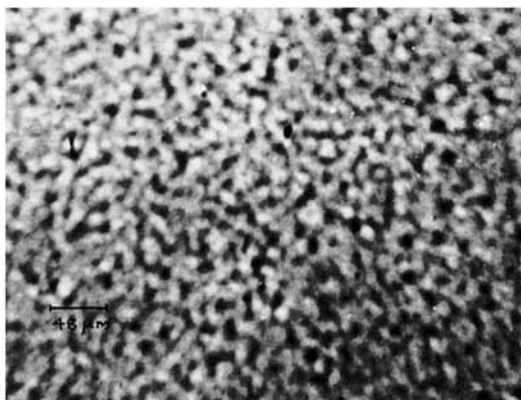
**Figure 3** (a) Scanning electron micrograph of the blend morphology of N<sub>30</sub> showing the dispersed nylon particles in the continuous NBR matrix. (b) Scanning electron micrograph of N<sub>50</sub> showing a co-continuous morphology. (c) Scanning electron micrograph of the blend morphology of N<sub>70</sub> where NBR particles are dispersed in nylon matrix.



(a)



(b)



(c)

**Figure 4** (a) Optical micrograph showing the surface morphology of  $N_{20}$ . (b) Optical micrograph showing the surface morphology of  $N_{40}$ . (c) Optical micrograph showing the surface morphology of  $N_{60}$ .

appears as large elongated structures that become drawn into domains. Upon further mixing, the elongated droplets are broken down into smaller spherical particles or droplets. To make proper correlation, it is necessary to have information about the morphological aspects, the nature of the matrix and the dispersed particles, the dimension and distribution of the dispersed particles, the extent and nature of the interfacial adhesion, etc. Therefore, in this study, SEM and optical microscopy are used to investigate the morphology of the blend system. The average particle size of the dispersed phase is found out by measuring the size of about 100 domains selected at random from the micrographs.

Figure 3(a)–(c) show the scanning electron micrographs of the fracture surface of the nylon-NBR blends having nylon nitrile rubber ratio 30/70, 50/50, and 70/30. In these blends, the NBR phase has been preferentially extracted using toluene. In Figure 3(b)–(c), the holes indicate the NBR phase that has been extracted by the solvent. Figure 4(a)–(c) shows the optical micrographs of the 20/80, 40/60, and 60/40 nylon-NBR blends. The two phases can be distinguished from the micrographs. The features of the blend system indicate an incompatible system. In nylon-rich blends, down to 60%, the dispersed phase is constituted by NBR. Thereafter, a continuum of the two components are observed down to

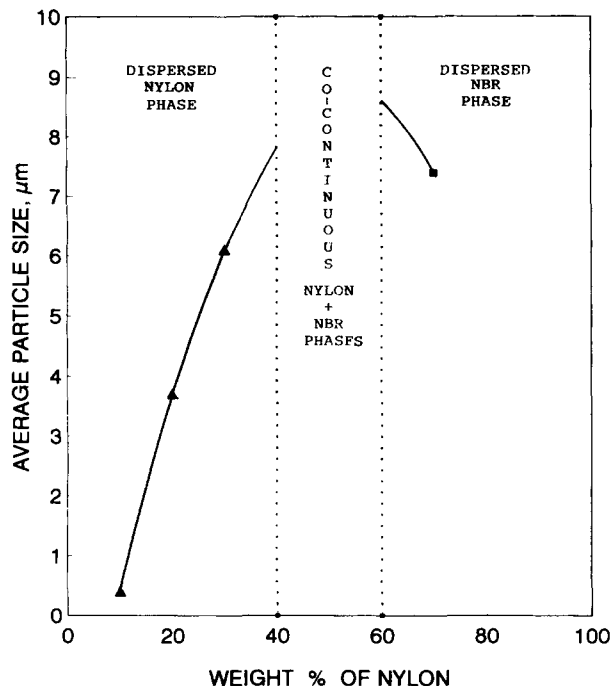


**Figure 5** Effect of blend composition on the dispersed particle size.

40% of the nylon. On further decrease of nylon concentration, nylon is found as the dispersed phase [Figs. 3(a) and 4(a)]. In NBR dispersed blend compositions, as the NBR content increases, the domain size increases. This is attributed to coarsening of NBR domains at higher concentration. The coalescent behavior of one of the components at higher concentration was reported by many authors.<sup>12,21,51,52</sup> The recombination of the dispersed domains has been reported at higher concentration of polyester in polyvinyl chloride/polyester blends by Thomas et al.<sup>51</sup> In  $N_{70}$  blend, the average particle size of the dispersed domains is  $7.3 \mu\text{m}$ . This can be understood from the micrographs. On the other hand, in  $N_{20}$  and  $N_{30}$  [Figs. 4(a) and 3(a)], nylon is the dispersed phase. In these cases, the average particle size varies from  $3.7$  to  $6.1 \mu\text{m}$ . In the cases of  $N_{40}$ ,  $N_{50}$ , and  $N_{60}$  [Figs. 4(b), 3(b), and 4(c)], both the phases exist as continuous phase. However, in these compositions, one can notice both dispersed and semicontinuous rubber phases. This indicates a nonuniform morphology. The average particle size versus composition is shown in Figure 5. In NBR-rich blends, the average particle size of the nylon domains are found to increase with increase in nylon concentration. Finally, a cocontinuous morphology is observed at 60/40, 50/50, and 40/60 compositions. The particle size distribution curve (Fig. 6) is drawn by measuring

the size of about 100 particles from the micrographs. The curve of  $N_{20}$  is having a narrow distribution. The broad distributions of  $N_{30}$  and  $N_{70}$  are attributed to the agglomeration of the nylon and NBR domains respectively due to their high concentration.

### Mechanical Properties

The stress-strain curves (Fig. 7) clearly picture the deformation nature of the samples under an applied load. The addition of noncrystalline elastomer phase in small concentration makes significant alteration in the load elongation curve. Blends of varying component ratio show different failure characteristics. Neat nylon and blends containing higher proportion of nylon ( $>50\%$ ) show high initial modulus. The stress-strain curves of these samples exhibit a well-defined yield at low elongation, indicating plastic deformation caused by the breakdown of continuous nylon matrix. In fact, the plots consist of two distinct regions. The curve up to the yield point shows clear elastic deformation; thereafter, the plastic deformation predominates. In the case of neat nylon, the sharp increase in stress with strain beyond the yield point is associated with the orientation of the crystalline hard segments of nylon. As the rubber content increases, the initial modulus and the yielding

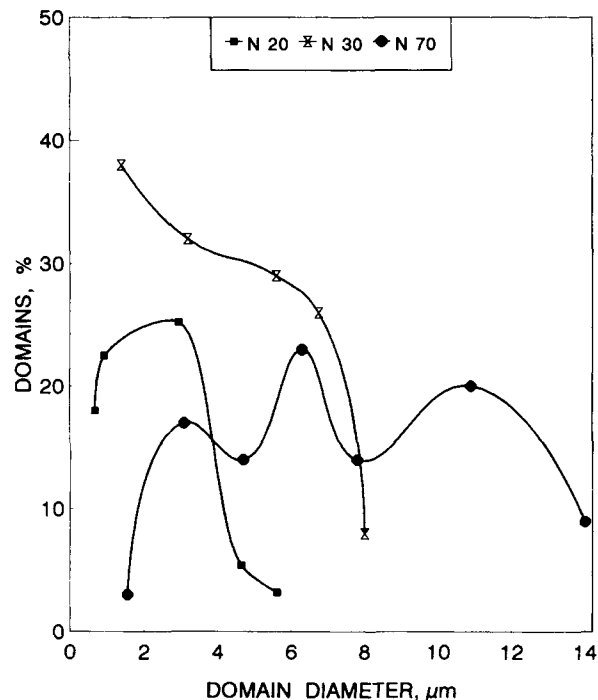


**Figure 6** Particle size distribution curve for the blend compositions  $N_{20}$ ,  $N_{30}$ , and  $N_{70}$ .

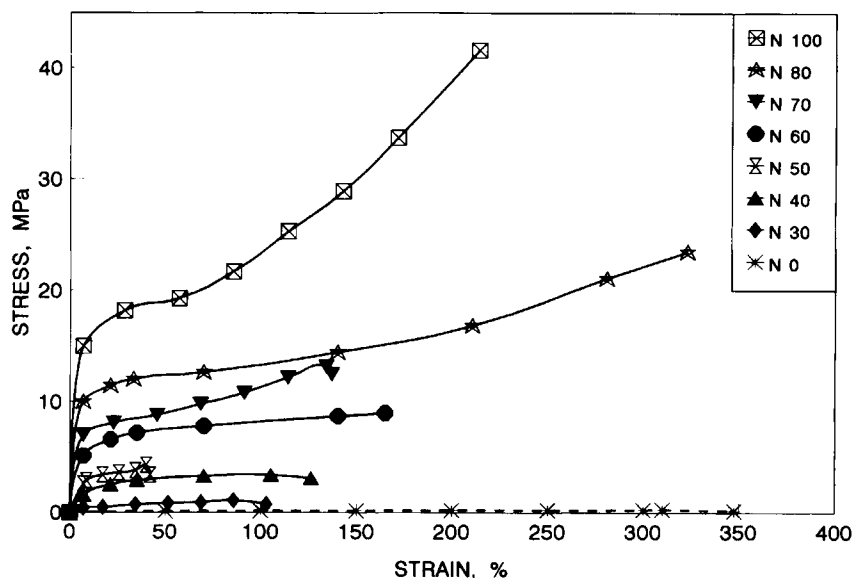


Figure 7 Stress-strain behavior of nylon/NBR blends having different blend ratios.

tendency decreases. The phase change morphology can be understood from stress-strain curves. The blends exhibit typical plastic behavior down to 70 weight percentage of nylon. This indicates that down to 70 weight percentage of nylon, NBR is the dispersed phase in a continuous nylon matrix. On further adding the NBR, the yield point disappears.  $N_0$  shows a stress-strain behavior that is typical of uncrosslinked elastomers. In case of  $N_{30}$  the stress initially increases slightly up to 85% elongation and then decreases until the failure occurs.  $N_{40}$ ,  $N_{50}$ , and  $N_{60}$  that are having a cocontinuous morphology exhibit a stress-strain behavior that is intermediate to those of the other blend compositions.

The tensile properties are important characteristics of polymers in general and crystalline polymers in particular. The tensile strength of the nylon-NBR blends depends on the strength of the nylon matrix, which in turn depends on the crystallinity of the nylon phase. Upon adding rubber, the crystallinity decreases and hence the properties associated with the long-range order also decreases. The crystallinity

of the samples have been analyzed using differential scanning calorimetry (DSC). The DSC analysis of the blends shows a decreasing trend of heat of fusion values of nylon with increasing NBR content. This suggests the decrease of crystallinity of the blends with increasing NBR. Therefore, the decrease of

Table II Heat of Fusion Values of the Blends

| Composition | Heat of Fusion Values (J/g deg.) |
|-------------|----------------------------------|
| $N_{100}$   | 3.12                             |
| $N_{70}$    | 2.58                             |
| $N_{60}$    | 2.28                             |
| $N_{40}$    | 1.21                             |

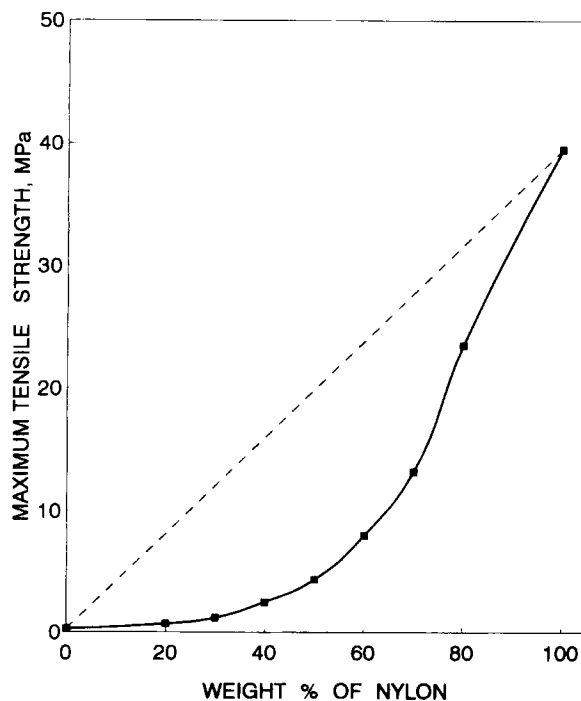
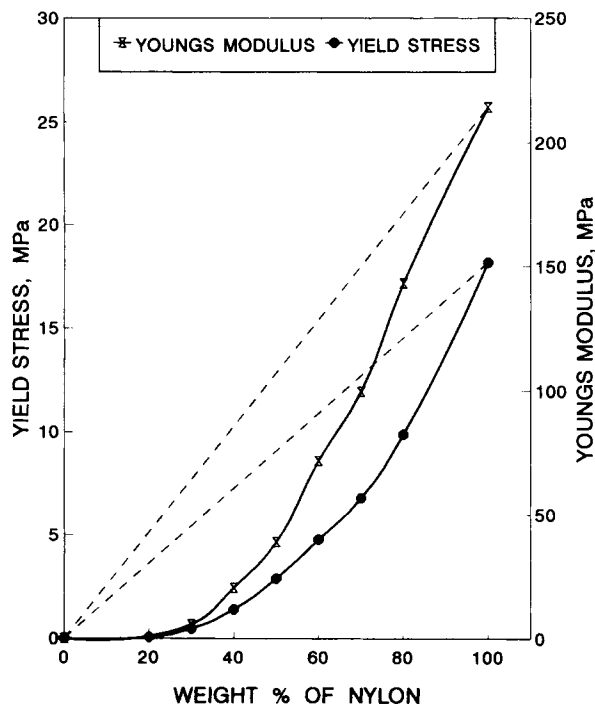


Figure 8 Effect of blend composition on maximum tensile strength.





**Figure 9** Effect of blend composition on the Young's modulus and yield stress of nylon/NBR blends.

mechanical properties with increase of NBR content is attributed to the decrease of crystallinity. The heat of fusion values are given in Table II. Earlier studies of Martuscelli et al.<sup>22</sup> and George et al.<sup>24</sup> have reported on the decrease of crystallinity of the plastic phase on the addition of the amorphous rubber.

The maximum tensile strength versus composition is shown in Figure 8, which shows a negative deviation. The reason is attributed to the poor interfacial adhesion between the highly crystalline nylon and amorphous nitrile rubber. The large voids seen on the fractured surface and the smooth surfaces from where the rubber particles are separated from the matrix clearly explain the poor interfacial adhesion between the two phases [Fig. 3(a)]. The voids have been formed as a result of debonding of the dispersed phase from the continuous matrix. Duvall et al.<sup>53</sup> have found similar observations in uncompatibilized nylon/polypropylene (PP) blends. In their study, the poor interfacial adhesion was evident from the large voids left on the fracture surface where the particles had separated from the matrix and thus smooth surfaces of the exposed PP particles. The failure stress depends considerably on the interfacial interaction between the two polymer phases. It is clear from Figure 8 that the tensile strength increases as the nylon content increases.

A sudden increase of tensile strength is seen in blends where the nylon concentration is greater than 40%. This sharp increase in tensile strength is associated with the predominance of the nylon phase as the continuous matrix.

The plots of Young's modulus and yield stress (Fig. 9) of nylon-NBR blends versus composition show a drastic reduction in their values as the rubber content in the blend increases. From Figure 9, it is clear that the Young's modulus increases considerably for blends of nylon weight percentage greater than 40. The curve has a negative deviation, as is seen from the figure. This is due to the high interfacial tension between the two phases and the low modulus values of NBR phase. From 40 weight percentage of nylon onward, the modulus increases remarkably due to the presence of high modulus nylon as continuous phase. The effect of percentage of nylon on elongation at break is given in Figure 10. The elongation at break is maximum for pure uncrosslinked NBR. The value decreases as the nylon content increases and is found to be lowest for 50/50 composition. Thereafter, the elongation at break is found to be increased. The low value of the elongation at break for the blends can be explained on the basis of the poor adhesion between the two phases in the blend. The tension set after failure

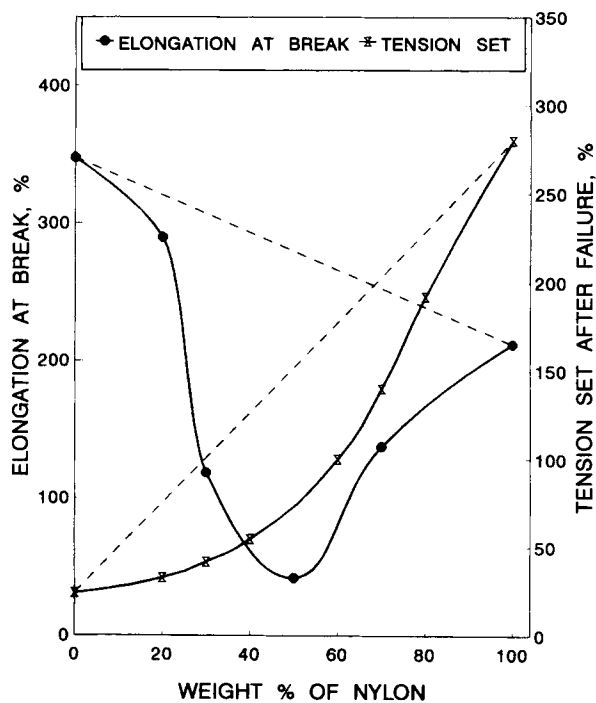


**Figure 10** Effect of blend composition on elongation at break and tension set of nylon/NBR blends.

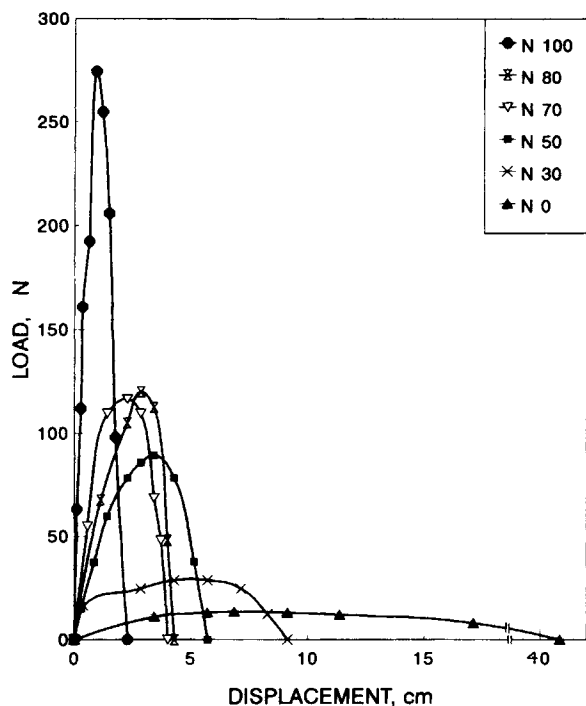


Figure 11 Tear curves of the nylon/NBR blends.

(Fig. 10) also increases as the plastic component increases. The considerable hike of tension set values for blends of high nylon content greater than 40% is attributed to the poor elastic recovery of the nylon phase after deformation.

The tear curves (load versus displacement) of the blends are given Figure 11. Nylon tears at the highest force and at the smallest displacement as observed in the figure. This shows the high resistance offered by nylon to tearing force. It is seen generally that the tearing force decreases and elongation increases as the amount of nylon decreases. Thus, NBR with the lowest tearing force shows highest elongation. The high elongation is attributed to the high extensibility of the uncrosslinked rubber phase upon stretching.

The effect of blend ratio on tear strength is shown in Figure 12. The tear strength decreases as the rubber content increases. Nylon is a crystalline plastic and NBR is an amorphous material of poor strength. Therefore, as the rubber content increases, the tear strength decreases. This is due to the decrease in crystallinity caused by the incorporation of elastomer phases. The tear strength values show a negative deviation. It is found from the Figure 12 that blends of high proportions of nylon (greater than 40 weight percentage) tear at higher force, and it can be understood that in these blends nylon behaves as a

continuous phase. The hardness of thermoplastic elastomeric blend has been tested and is reported in shore D units (Fig. 12). The values change from 38 shore D for pure nylon to 1 shore D for N<sub>30</sub>. In this case, the curve has a positive deviation because the hardness is inherently a surface property and is much less dependent on the interfacial adhesion.

#### Effect of Testing Speed on Mechanical Properties

Figure 13 shows the stress-strain curves of 50/50 nylon/NBR blend at various strain rates such as 5, 50, and 500 mm/min. The three curves show similar behavior. Most of the mechanical properties like tensile strength, Young's modulus, yield strength, and tear strength are maximum when the testing is done at a crosshead speed of 500 mm/min (Fig. 14). It is well recognized that the value of tensile strength and Young's modulus of polymeric materials become greater as strain rate increases because of their viscoelastic nature. The ultimate elongation is found to be less at higher strain rates as expected. The accumulated stress in polymer material required to produce some microcrazes in it (some of the crazes will grow to be cracks and cause of fracture) is considered to be constant. To avoid the fracture of the material under increased strain ratio, these stresses should be relieved through some dissipation of en-

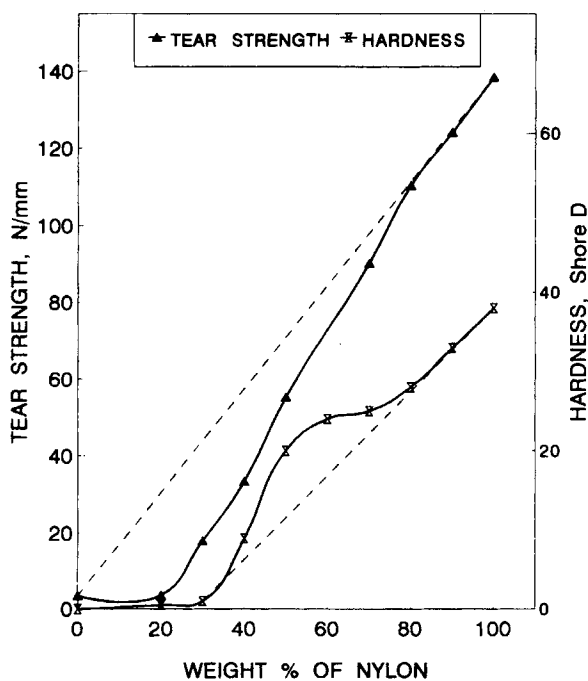


Figure 12 Effect of blend composition on the tear strength of nylon/NBR blends.

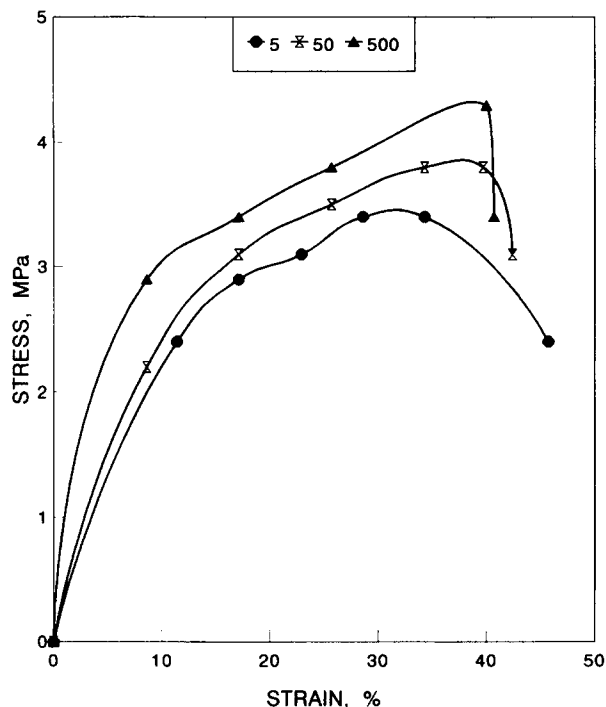


Figure 13 Effect of strain rates on the stress-strain behavior of 50/50 blend composition.

ergy, such as yielding or necking. Rubber incorporation is found to be effective for this purpose. In the present case, the curves show high initial modulus followed by a necking tendency at the fracture point. When the apparent tensile stress increases under increased deformation rate, the possibility for the relief of the involved stress becomes less and the fracture should occur at less strain position. This accounts for the decrease of elongation at high strain rate. The general explanation offered for the tensile behavior of viscoelastic materials under varying strain rate is as follows. Polymer chains can be considered as entangled random coils that pass through the cross-section of the test piece. At the instant stress is applied to the sample, each segment that passes through the cross-section aids in supporting the stress. As time goes on (i.e., decreasing the crosshead speed), the chain elongates fully, and there will be fewer segment passing through the cross section. This process of decoiling and chain straightening continue until the polymer chain is fully elongated and only one of the segments will hold the load in the cross-section under consideration. This will result in the poor strength of the material. On the other hand, at high testing speed, the decoiling and chain straightening is negligible. Therefore,

large number of segments will hold the applied load. This will result in a high strength of the material.

**Theoretical Modeling**

Applicability of various models such as Parallel, Series, Halpin-Tsai, and Coran's equations has been examined to predict the tensile strength, tear strength, and the Young's modulus of these blends. The upper bound of modulus is given by the rule of mixtures.

$$M = M_1\phi_1 + M_2\phi_2 \tag{1}$$

In the above equation,  $M$  is the modulus of the blend and  $M_1$  and  $M_2$  are the moduli of the components 1 and 2, respectively.  $\phi_1$  and  $\phi_2$  represent the volume fraction of the component 1 and 2, respectively. This equation is applicable for models in which the components are arranged parallel to the applied stress. The lower bound to the modulus holds for models in which the components are arranged in series with the applied stress and the equation for this is

$$1/M = \phi_1/M_1 + \phi_2/M_2 \tag{2}$$

According to Halpin-Tsai equation

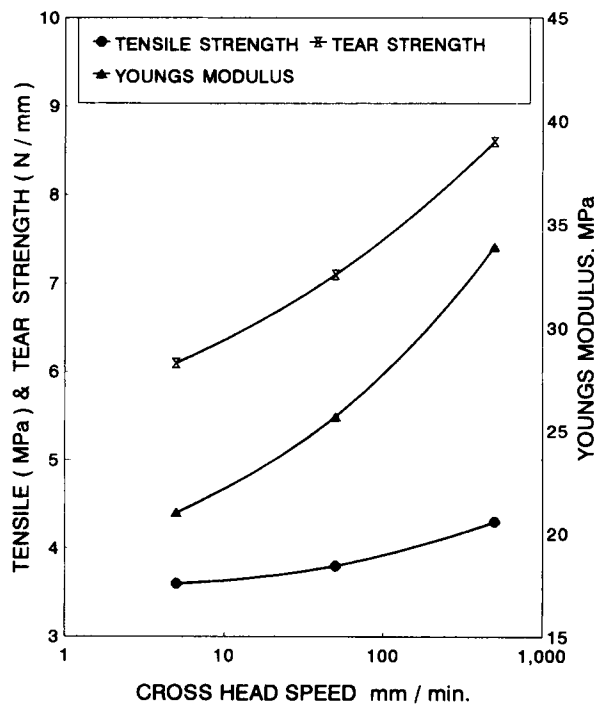


Figure 14 Effect of strain rates on the mechanical properties of 50/50 nylon/NBR blends.

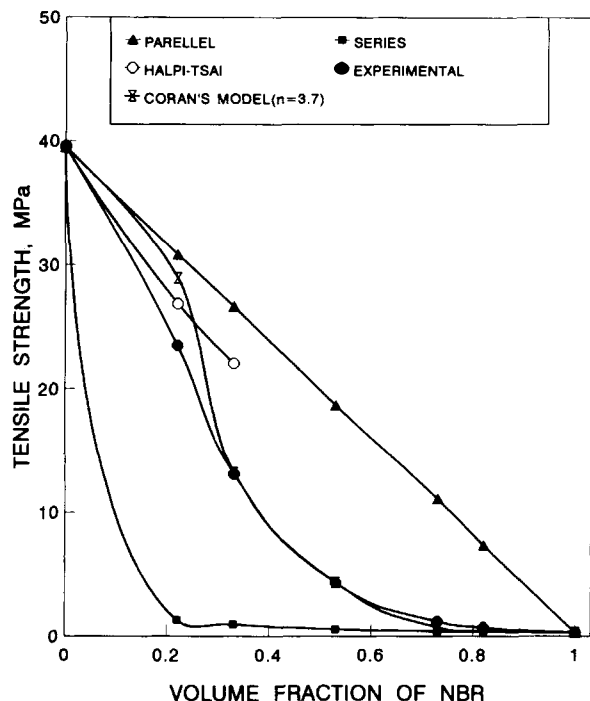


Figure 15 Applicability of various models on the tensile strength of the blends.

$$M_1/M = (1 + A_i B_i \phi_2)/(1 - B_i \phi_2) \quad (3)$$

where  $B_i = (M_1/M_2 - 1)/(M_1/M_2 + A_i)$ . In the Halpin-Tsai equation, subscripts 1 and 2 represent the continuous and dispersed phase, respectively. The constant  $A_i$  is defined by the morphology of the system. For elastomer domains dispersed in continuous hard matrix,  $A_i = 0.66$ .

According to Coran's equation,

$$M = f(M_U - M_L) + M_L \quad (4)$$

where  $f$  can vary between zero and unity. The value of  $f$  is a function of phase morphology. The values of  $f$  is given by

$$f = V_H^n / (nV_S + 1) \quad (5)$$

where  $n$  contains the aspects of phase morphology.  $V_H$  and  $V_S$  are in the volume fractions of hard phase and soft phase, respectively. The change in  $f$  with respect to  $V_H$  is greatest when  $V_H = (n - 1)/n$ . Thus, the value of  $(n - 1)/n$  could be considered as the volume fraction of hard phase material that corresponds to a phase inversion.

Figures 15–17 show the experimental and theoretical curves of mechanical properties (tensile

strength, tear strength, and Young's modulus) as a function of soft-phase volume fraction. It can be seen from these figures that experimental data are very close to the Coran's model in which the value of  $n = 3.7$ . The value  $n - 1/n$  corresponds to  $V_H = 0.729$  as the hard-phase volume fraction that corresponds to a phase inversion of NBR from dispersed phase to continuous phase. This result is almost consistent with our experimental results from morphology and mechanical properties studies.

## CONCLUSION

Morphology of nylon-NBR blends indicates a two-phase structure in which NBR is dispersed as domains in the continuous nylon phase at lower proportions, but as the proportion of the rubber increases beyond 40%, this component also exists as a continuous phase. It is found that the minor component appears as the dispersed phase, and its domain size increases with increase of its concentration. The morphology of the blend is found to have a strong influence on the mechanical properties. The mechanical properties are found to increase rapidly beyond 40 wt % of nylon. This abrupt rise in mechanical properties is associated with the fully con-

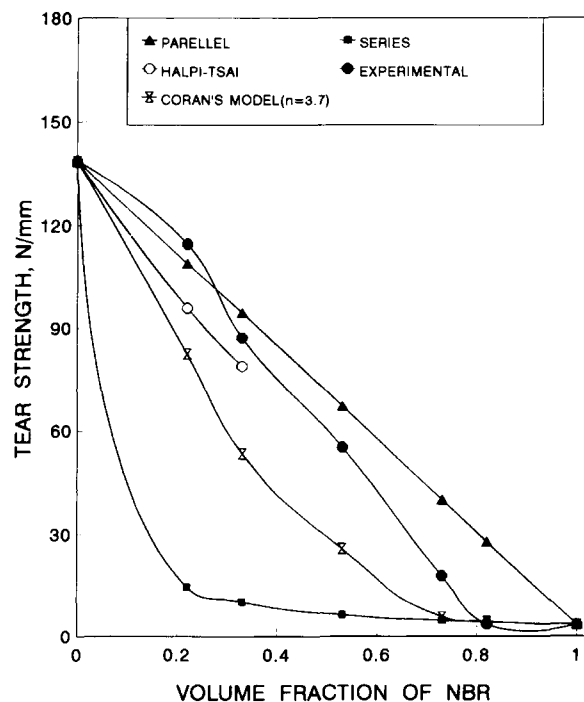
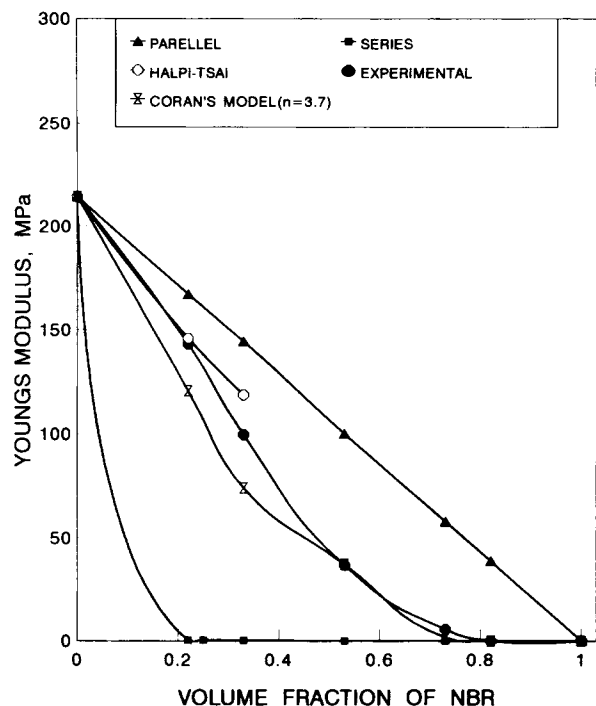


Figure 16 Applicability of various models on tear strength of the blends.



**Figure 17** Applicability of various models on Young's modulus of the blends.

tinuous nature of the nylon matrix. Mechanical properties such as tensile strength, Young's modulus, tear strength, hardness, and tension set are higher for blends containing higher proportions of nylon. The modulus also is found to be maximum for composition of higher plastic content. Almost all properties are found to decrease with the addition of NBR, which is due to the reduced crystallinity of the nylon and also due to the poor interfacial interaction at the blend interface. Almost all the mechanical properties except hardness are found to have a negative deviation. The influence of strain rate on the mechanical properties have been analyzed. The properties like tensile strength, tear strength, and Young's modulus are maximum when the testing speed is 500 mm/min. Various theoretical models have been used to predict the tear strength, tensile strength, and Young's modulus of the blends. It is found that the Coran's and Halpin-Tsai model fit the experimental results.

## REFERENCES

1. B. M. Walker, *Hand Book of Thermoplastic Elastomers*, Van Nostrand Reinhold Company, New York, 1979.

2. A. D. Thorn, *Thermoplastic Elastomers, A Review of Current Information*, Rubber and Plastics Research Association of Great Britain, Shawbury, England (1980).
3. J. C. West and S. L. Cooper, *Science and Technology of Rubber*, F. R. Eirich, Ed., Academic Press, Inc., New York, Ch. 13, 1978.
4. A. Whelan and K. S. Lee, *Developments in Rubber Technology 3, Thermoplastic Rubbers*, Applied Science Publishers, London, 1982.
5. L. Mullins, *Rubber Dev.*, **31**, 92 (1978).
6. T. J. Nelson and N. Subramanian, *Polym. Intern.*, **32**, 343 (1993).
7. S. Wu, *Polymer*, **26**, 1855 (1985).
8. A. Margolina and S. Wu, *Polymer*, **29**, 2170 (1988).
9. T. Fulkui, Y. Kikuchi, and T. Inoue, *Polymer*, **33**, 3173 (1992).
10. Y. Takeda, H. Keskkula, and D. R. Paul, *Polymer*, **33**, 3173 (1992).
11. S. Danesi and R. S. Porter, *Polymer*, **19**, 448 (1978).
12. K. C. Dao, *Polymer*, **25**, 1527 (1984).
13. M. Baer, *J. Appl. Polym. Sci.*, **16**, 1109 (1972).
14. C. G. Bragaw, *Advances in Chemistry*, ACS Symposium Series 99, American Chemical Society, Washington, D.C., 1971.
15. W. M. Speri and G. R. Particle, *Polym. Eng. Sci.*, **15**, 668 (1975).
16. C. K. Riew, E. H. Rowe, and A. R. Stebert, *Advances in Chemistry*, ACS Symposium Series 154, American Chemical Society, Washington, D.C., 1976.
17. S. Miller, *TIS Report 78 MAL005*, General Electric Company, Louisville, KY, 1978.
18. S. Miller, *Proceedings Int. Conf. Toughening of Plastics*, Paper 8, Plastics and Rubber Institute, London, 1978.
19. S. Cimmino, L. D'Orazio, R. Greco, G. Maglio, M. Malinconica, C. Mancarell, E. Murtuscelli, R. Palumbo, and G. Ragosta, *Polym. Eng. Sci.*, **24**, 48 (1984).
20. D. Yang, B. Zhang, Y. Yang, Z. Fang, G. Sun, and Z. Feng, *Polym. Eng. Sci.*, **24**, 612 (1984).
21. D. Heikens and W. Barentsen, *Polymer*, **18**, 69 (1977).
22. E. Murtuscelli, C. Silvestre, and G. Abate, *Polymer*, **23**, 229 (1982).
23. E. Murtuscelli, F. Riva, C. Sellitti, and C. Silvestre, *Polymer*, **26**, 270 (1985).
24. S. George, K. T. Varughese, and S. Thomas, *Polymer*, to appear.
25. K. C. Dao, *Polymer*, **25**, 1527 (1984).
26. M. Baer, *J. Appl. Polym. Sci.*, **16**, 1109 (1972).
27. R. J. M. Borgreve, R. J. Gaymans, J. Schuijjer, and J. F. Insen Housz, *Polymer*, **28**, 1489 (1987).
28. R. J. Gaymans, R. J. M. Borgreve, and A. B. Spoelstra, *J. Appl. Polym. Sci.*, **37**, 479 (1989).
29. R. J. M. Borgreve and R. J. Gaymans, *Polymer*, **30**, 63 (1989).

30. R. J. M. Borgreve, R. J. Gaymans, and J. Schuijjer, *Polymer*, **30**, 71 (1989).
31. A. Y. Coran and R. P. Patel, *Rubber Chem. Technol.*, **53**, 141 (1980).
32. A. Y. Coran and R. P. Patel, *Rubber Chem. Technol.*, **54**, 91 (1981).
33. A. Y. Coran and R. P. Patel, *Rubber Chem. Technol.*, **53**, 781 (1980).
34. A. Y. Coran and R. P. Patel, *Rubber Chem. Technol.*, **54**, 892 (1981).
35. A. Y. Coran and R. P. Patel, *Rubber Chem. Technol.*, **55**, 116 (1982).
36. B. Kuriakose and S. K. De, *Polym. Eng. Sci.*, **25**, 630 (1985).
37. B. Kuriakose and S. K. De, *Mater. Chem. Phys.*, **12**, 157 (1985).
38. B. Kuriakose and S. K. De, *J. Mater. Sci. Lett.*, **4**, 455 (1985).
39. S. Akhtar, P. P. De, and S. K. De, *Mater. Chem. Phys.*, **12**, 235 (1985).
40. S. Thomas, S. K. De, and B. R. Gupta, *Kautsch. Gummi Kunst.*, **40**, 665 (1987).
41. S. Thomas, B. Kuriakose, B. R. Gupta, and S. K. De, *J. Mater. Sci.*, **21**, 711 (1986).
42. S. Thomas, B. R. Gupta, and S. K. De, *Polym. Degrad. Stab.*, **18**, 189 (1987).
43. S. Thomas, B. R. Gupta, and S. K. De, *J. Mater. Sci.*, **22**, 3209 (1987).
44. S. Thomas, *Mater. Lett.*, **5**, 9 (1987).
45. A. T. Koshy, B. Kuriakose, S. Thomas, and S. Varghese, *Polymer*, **34**, 16, 3428 (1993).
46. A. T. Koshy, B. Kuriakose, S. Thomas, C. K. Premalatha, and S. Varghese, *J. Appl. Polym. Sci.*, **49**, 901 (1993).
47. S. S. Dagli, N. Xanthos, and J. A. Beisenberger, *Polym. Eng. Sci.*, **34**, 1723 (1994).
48. C. E. Scott and C. W. Macosko, *Polymer*, **35**, 5425 (1994).
49. G. N. Avegeropoulos, F. L. Weissert, P. H. Biddison, and G. G. A. Bohn, *Rubber Chem. Technol.*, **49**, 93 (1976).
50. G. R. Hamed, *Rubber Chem. Technol.*, **55**, 151 (1982).
51. S. Thomas, B. R. Gupta, and S. K. De, *J. Vinyl Technol.*, **9**, 71 (1987).
52. Z. K. Wakzak, *J. Appl. Polym. Sci.*, **17**, 169 (1973).
53. J. Duvall, C. Sellitti, V. Topolkaraev, A. Hiltner, E. Baer, and C. Myers, *Polymer*, **35**, 3948 (1994).

Received July 20, 1995

Accepted April 9, 1996